Thin Solid Films 520 (2012) 4726–4729

Contents lists available at SciVerse ScienceDirect

Thin Solid Films

journal homepage: www.elsevier.com/locate/tsf

Investigation on indium concentration dependence of solution processed indium tin oxide thin film transistors

C.H. Jung [a], J.Y. Lee [a], L.S. Pu [b], K.S. Lee [c], D.H. Yoon [a,d,*]

[a] SKKU Advanced Institute of Nanotechnology (SAINT), Sungkyunkwan University, Suwon 440-746, Republic of Korea
[b] AMPIT, Sungkyunkwan University, Suwon 440-746, Republic of Korea
[c] School of Information and Communication Engineering, Sungkyunkwan University, Suwon 440-746, Republic of Korea
[d] School of Advanced Materials Science & Engineering, Sungkyunkwan University, Suwon 440-746, Republic of Korea

ARTICLE INFO

Available online 10 November 2011

Keywords:
Indium tin oxide
Thin film transistor
Solution process
Mobility

ABSTRACT

The effect of the indium content in indium tin oxide (ITO) films fabricated using a solution-based process and ITO channel thin film transistors (TFTs) was examined as a function of the indium mole ratio. The carrier concentration and resistivity of the ITO films could be controlled by the appropriate treatments. The TFTs showed an increase in the off-current due to the enhanced conductivity of the ITO channel layer with increasing indium mole ratios, producing an increase in the field effect mobility. The characteristics of the a-ITO channel TFT showed the best performance (μ_{FE} of 3.0 $cm^2 V^{-1} s^{-1}$, V_{th} of 2.0 V, and S value of 0.4 V/decade) at In:Sn = 5:1.

1. Introduction

Recently, zinc oxide (ZnO) based oxide materials have attracted considerable attention for a range of applications, such as transparent conducting oxides, solar cells, sensor and thin film transistors. In particular, amorphous oxide semiconductors (AOSs) thin film transistors (TFTs) offer attractive alternatives to amorphous Si TFTs owing to their high mobility and reasonable on–off ratio at low temperatures [1–4]. Among the AOSs composed of heavy metal cations with $(n\text{-}1)d^{10}ns^0$ ($n \geq 5$) electronic configurations, which show improved electron transport because the ns^0 orbitals form large overlap with cations [5–7], amorphous indium gallium zinc oxide (IGZO) and zinc tin oxide (ZTO) have been reported as the channel layer in TFTs. However, most of these oxide semiconductor channel TFTs are fabricated by vacuum processes, such as radio frequency magnetron sputtering, atomic layer deposition, and pulsed laser deposition.

For large-area flat panel display applications, solution processes with low cost, accurate composition control and high throughput, such as spin-coating, printing and roll-to-roll processing, can be the best breakthrough compared to conventional vacuum processes. Recently, several groups reported that amorphous ZnO [8], ZTO [9], IGZO [10,11] and indium zinc oxide [12] in TFTs as a active channel layer could be fabricated using a spin-coating process and showed reasonable performance such as excellent field effect mobility, improved bias stress instability due to the control of high gate insulators and additive dopants, compared to conventional vacuum processed TFTs. This study investigated the electrical and structural properties of solution processed amorphous indium tin oxide (a-ITO) films as a function of indium mole ratio, and examined effect of the indium mole ratios of a-ITO channel TFTs on their properties. The electrical properties of a-ITO films and a-ITO channel TFTs fabricated by solution process as a function of indium mole ratio are also discussed.

2. Experimental details

The precursor solution for fabricating thin films was prepared by dissolving indium chloride ($InCl_3$) and tin chloride ($SnCl_2$) powders in 2-methoxyethanol ($CH_3OCH_2CH_2OH$). To form a stable solution, the precursor was chelated with monoethanolamine ($NH_2CH_2CH_2OH$). The solution was stirred at room temperature for 1 h to produce a transparent and homogeneous solution. The indium (In):tin (Sn) mole ratio was varied from 1:1 to 9:1. After a sufficient reaction, the solution was filtered through a 0.22 μm syringe filter and spin-coated at a speed of 3000 rpm for 30 s on a top a SiO_2/Si (heavily *n*-type doped) substrate. After spin-coating, the films were dried at 80 °C for 10 min, and annealed from 300 to 500 °C for 10 min by a furnace in air or nitrogen atmosphere and cooled to room temperature.

The 200-nm-thick SiO_2 gate insulator of the TFTs was thermally grown on Si substrates followed by the deposition of a 100-nm-thick Al film on the backside of Si substrate by E-beam evaporation to form the gate electrode. The a-ITO channel layers were deposited with different indium mole ratios using spin-coating process and annealed at 500 °C for 1 h in an oxygen atmosphere. The 100-nm-thick source/drain electrodes (Al) were e-beam evaporated on top of the channel layer. The channel width (W) and length (L) were 800 μm and 100 μm, respectively. The thermal decomposition

* Corresponding author at: SKKU Advanced Institute of Nanotechnology (SAINT), Sungkyunkwan University, Suwon 440-746, Republic of Korea. Tel.: +82 31 290 7361; fax: +82 31 290 7371.
E-mail address: dhyoon@skku.edu (D.H. Yoon).

0040-6090/$ – see front matter © 2011 Elsevier B.V. All rights reserved.
doi:10.1016/j.tsf.2011.10.187

behavior was observed by thermogravimetric analysis (Seiko Exstar 6000, SEICO) in air. The structural properties of the a-ITO films were analyzed by field emission scanning electron microscopy (FESEM, JSM-7500F, JEOL) operating at an accelerating voltage of 5–15 kV, high resolution transmission electron microscopy (HRTEM, JEM-2100F, JEOL) operating at an accelerating voltage of 300 kV and synchrotron X-ray scattering, respectively. The cross-sectional HRTEM samples were prepared by mechanical polishing with diamond polishing papers, and then made into thin sections with Ar-ion milling. The synchrotron scattering experiments were performed at beamline 3C2 with Cu $K_{\alpha 1}$ radiation (1.54 Å) at the Pohang Light Source (PLS) in Korea. The surface roughness of the film was characterized with atomic force microscopy (Innova, Veeco) in tapping mode at a slow scanning rate (scan speed of 0.5–1.0 Hz). To obtain high resolution images, super sharp silicon probes (NANOWORLD, NCHR-50) were used to capture the image. The carrier concentration and resistivity of the films were measured using the Van der Pauw configuration in a magnetic field of 0.55 T at room temperature. The electrical properties of the TFTs were examined in air at room temperature using a Keithley 4200 semiconductor characterization system.

3. Results and discussion

Thermal analysis of the ITO solution indicated that the weight loss of the ITO solution occurred in three steps, as shown in Fig. 1(a). The initial weight loss was approximately 30% at 150 °C due to the removal of solvent and surface moisture. The additional weight loss in two steps was attributed to the decomposition of indium chloride and tin chloride up to 400 °C, respectively. This suggests that an annealing temperature of 400–500 °C would be sufficient for the formation of the ITO films. Fig. 1(b) shows synchrotron X-ray diffraction patterns of ITO films after annealing at different temperatures from 300 to 500 °C. All films were amorphous irrespective of the annealing temperature. For the detained investigation of films, the HRTEM image and fast Fourier transform (FFT) pattern of the ITO film annealed at 500 °C were examined as shown in Fig. 1(c). The HRTEM image and FFT pattern showed clearly amorphous phase and uniformly fabricated ITO films.

Fig. 2(a) shows a cross-sectional FESEM image of the ITO film deposited on a SiO_2/Si substrate by spin-coating followed by annealing at 500 °C. The spin-coated film was highly dense with no grain shape or column structure. In addition, the plane FESEM image showed that the surface smoothness of the film was clear and uniform, indicating no grains or grain boundaries due to the amorphous phase, as shown in Fig. 2(b). The surface roughness of the a-ITO film was approximately 1.0 nm (data not shown). These results are consistent with the synchrotron scattering results, indicating that the ITO film annealed at 500 °C was amorphous structure, as shown in Fig. 1(b) and (c).

The electrical properties of the ITO films deposited as a function of the indium mole ratio were examined by Hall measurements. The carrier concentration and resistivity of all the ITO films varied from 6.5×10^{12} to 1.9×10^{19} cm^{-3} and 6.3×10^{4} to 3.1×10^{-4} Ω cm with increasing indium content, respectively, as shown in Fig. 3(a) and (b). In addition, the ITO films annealed with increasing temperature from 400 to 500 °C and in a N_2 nitrogen atmosphere showed a sudden change from insulating to semiconducting behavior. This suggests that the electrical properties of the ITO film are affected by the indium content, as well as the annealing temperature and ambient atmospheres, which is related to the number of oxygen vacancies. The increase in the number of oxygen vacancies leads to an increase in carrier concentration and a decrease in resistivity because oxygen vacancies create free electrons in the films. From these results, the carrier concentration and resistivity of the ITO films can be controlled for commercial applications through the appropriate treatments.

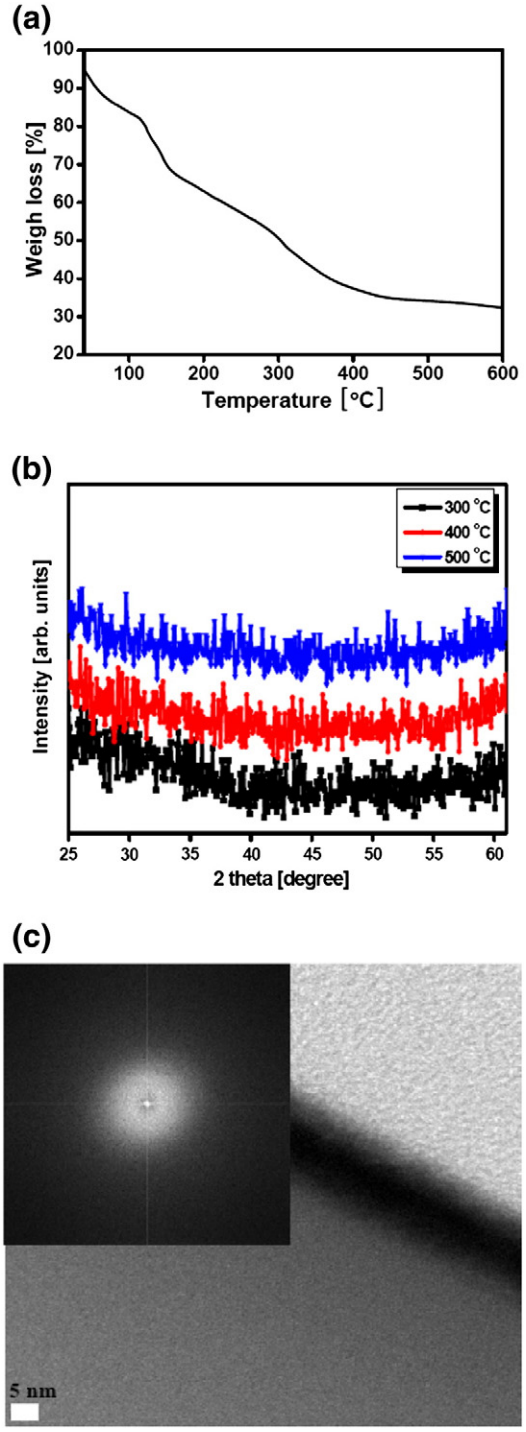

Fig. 1. (a) Thermogravimetric curve of the ITO solution, (b) synchrotron X-ray diffraction patterns of amorphous ITO films with increasing annealing temperature from 300 to 500 °C, and (c) HRTEM image and FFT pattern of the ITO films annealed at 500 °C.

Fig. 4 shows the drain current versus gate voltage (I_{DS}–V_{GS}) of 15 V transfer characterization of the ITO films with increasing indium mole ratios. The solution processed a-ITO channel TFT exhibit typical n-channel transistors characteristics with good gate modulation, hard saturation and a high on-current. The threshold voltage (V_{th}) and field effect mobility (μ_{FE}) of the device was approximated by a linear extrapolation of the curve using the following equation:

$$I_{DS} = \left(\frac{\mu_{FE} W \varepsilon_0 \varepsilon_r}{2Ld}\right)(V_{GS} - V_{th})^2 \quad (1)$$